

PAPER

[View Article Online](#)
[View Journal](#) | [View Issue](#)Cite this: *Catal. Sci. Technol.*, 2021, 11, 4529

Synthesis of a H-Sulfo-POSS catalyst and application in the acetalization of glycerol with 2-butanone to yield a biofuel additive†

Viktor Söderholm,^a Jesús Esteban ^b and Dieter Vogt ^{*a}

Nanosized polyhedral oligomeric silsesquioxanes (POSS) have been employed as molecular weight enlarged structures for different purposes owing to their ease of synthesis and modification. In this work, the commercially available compound octaphenyl-POSS has been modified with chlorosulfonic acid to obtain multifunctional acidic materials (H-Sulfo-POSS) with different degrees of functionality in the structure. The synthesized materials have been characterized by ion exchange capacity, degree of sulfonation, ¹H-NMR, ATR-IR spectroscopy and SEM. These H-Sulfo-POSS nanocomposites were then applied to the acetalization of glycerol with 2-butanone to yield the corresponding ketal, which is a product of interest as an oxygenate fuel additive. The catalytic activity in dynamic experiments of the H-Sulfo-POSS (2601 h⁻¹) material with the highest degree of sulfonation was even higher than that shown by the molecular catalyst *para*-toluene sulfonic acid (PTSA) (2256 h⁻¹) and better than Amberlyst 36 (213 h⁻¹); however, upon recycling by centrifugation of the catalyst, the activity of this material was not very stable. On the other hand, the material with the lowest degree of sulfonation showed not only higher activity than Amberlyst 36, but also very stable activity after reutilization throughout 10 runs.

Received 25th February 2021,
Accepted 24th May 2021

DOI: 10.1039/d1cy00344e

rsc.li/catalysis

1. Introduction

Silsesquioxanes are hybrid inorganic–organic nanostructured materials that are gaining increasing attention as advanced polymer composites. They originate from the hydrolysis and condensation of silanes with alkoxy groups and can acquire different structures like ladder, cage and partial cages. Polyhedral oligomeric silsesquioxanes (POSS) have become very attractive arrangements of silsesquioxanes that originate from different monomers giving rise to structures of the general formula (RSiO_{1.5})_n, in which R can be a range of organic substituents that lead to styryl-POSS, methacrylate-POSS, norbornyl-POSS, vinyl-POSS, epoxy-POSS or siloxane-POSS, among others.^{1,2} Fig. 1 presents the general structure of a cubic POSS material.

Owing to their environmental neutrality, chemical and thermal inertness, high heat resistance features and ability to improve mechanical properties of polymers, they have been widely applied. Many studies have studied POSS or POSS-containing hybrid polymers as fire retardants, high

performance materials in nanocomposite membranes or in the synthesis of advanced materials for biomedicine and tissue engineering, electronics or photo- and electroluminescence devices.^{2–4}

POSS have also seen applications in catalysis owing to their characteristic arrangements, rigid structure and commercial availability, which make them great candidates for molecular weight enlargement (MWE), with the corresponding good recyclability features. For example, a POSS-supported N-heterocyclic carbenes/imidazolium salts

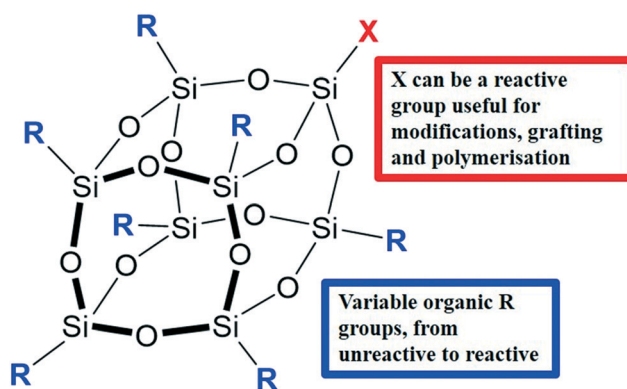


Fig. 1 The general structure of a cubic polyhedral oligomeric silsesquioxane (POSS). Organic R groups can be unreactive or reactive, with the X substituent being different or the same as R.

^a Laboratory of Industrial Chemistry, Department of Biochemical and Chemical Engineering, Technical University of Dortmund, Emil-Figge-Str. 66, D-44227 Dortmund, Germany. E-mail: dieter.vogt@tu-dortmund.de

^b Department of Chemical Engineering and Analytical Science, The University of Manchester, Manchester M13 9PL, UK

† Electronic supplementary information (ESI) available. See DOI: 10.1039/d1cy00344e

on Pd nanoparticles have proven effective and recyclable catalysts for Suzuki–Miyaura cross-coupling reactions with TOFs as high as 1670 h^{-1} .⁵ Another case is the use of hybrid composites made from octa-aminopropyl POSS hydrochloride salt and ionic liquids onto which Cu or Ag nanoparticles are immobilized. Such catalysts are active and show good recyclability in “click” reactions and in the reduction of 4-nitrophenol.⁶ Finally, the catalytic activity of Ru complexes, molecular weight enlarged by POSS moieties, in metathesis reactions proved comparable to that of commercially available second generation Grubbs–Hoveyda catalysts. Recycling experiments proved that the retention of the catalyst was high when separating the product with ceramic membranes.⁷

As a consequence of the development of the biodiesel industry, over the years, glycerol (Gly) has become widely available and there has been an opportunity to use it as a building block for many products of interest.^{8,9} Among them, glycerol acetals appear as interesting additives in (bio)fuels owing to their oxygenate nature, which have rendered them useful as enhancers of the octane number and cold flow properties as well as successfully reducing particulate emissions and gum formation.^{10,11}

The production of glycerol acetals stems from the acid-catalyzed reaction of glycerol with aldehydes or ketones in a reaction that also generates a molecule of water as a by-product. The reaction will only take place in the presence of an acid catalyst.^{10,11} The acetal products obtained in this reaction can contain 5-membered rings (dioxolanes) or 6-membered rings (dioxanes), the former being usually kinetically favoured. Fig. 2 presents a scheme of the reaction.

Different catalysts have been used for this purpose. PTSA has been utilized for the acetalization of glycerol with formaldehyde,¹² acetone¹³ or benzaldehyde.¹⁴ As for heterogeneous catalysts, sulfonic acid-based ion exchange resins like the classic Amberlyst 15 have been used for the reaction of glycerol with aldehydes of different chain length from butanal to decanal,¹⁵ Amberlyst 35 and 36 for the production of solketal with acetone^{16,17} or reacting glycerol with formaldehyde or benzaldehyde.¹⁸ Other solid materials include micro or mesoporous materials like zeolites, such as USY or ZSM for reaction with butanal¹⁹ or BEA with benzaldehyde,¹⁸ or montmorillonite K-10.¹⁸

Finally, a polystyrene sulfonate-octavinyl POSS polymeric catalyst (POSS-*x*-SO₃H) has been successful used in the acetalization of glycerol with benzaldehyde, reaching

conversions over 92% with good overall selectivity to the acetal products.²⁰ Moreover, the selectivity to the dioxolane product with respect to the dioxane was 72:20,²⁰ higher than those obtained with Amberlyst 36 (61:39), zeolite BEA (59:41) or montmorillonite K-10 (48:52).¹⁸ The reaction with butanone is also possible, but has been somehow understudied considering the similarity of the product with solketal. For this reaction, focus of our present study, there are reports using the following catalysts: H₃PW₁₂P₄₀,²¹ SnCl₂,²² AlF₃·H₂O,²³ and Re/SiO₂.²⁴

Given the use of acidic catalysts for this reaction and others involving renewable substrates to further value-added chemicals, materials modified with sulfonic acid functionalities appear as an interesting alternative. Another example of reaction requiring acidic media to take place is the dehydration of sugars like glucose or fructose to obtain 5-hydroxymethylfurfural and levulinic acid,²⁵ which has been reported using a sulfonated hyperbranched poly(arylene oxindole) as catalyst.²⁶ In this sense, H-Sulfo-POSS poses a multifunctional nanomaterial that could be of interest for catalysis. Therefore, this work focuses on the synthesis of this material, its characterization and performance in the acetalization of glycerol, also analyzing its stability upon several cycles of recycling.

2. Experimental

2.1. Materials

For the preparation of the H-Sulfo-POSS catalysts, the following chemicals were used: OP-POSS (Hybrid Plastics, 99%), chlorosulfonic acid (Acros Organics, 97%), dichloromethane (VWR, 99.5%) and chloroform (VWR, 99.8%). The catalytic runs for the synthesis of the glycerol acetal required the use of glycerol (Henkel, 99%), butanone (Aldrich, 99%), ethanol (ITW Reagents, 99%), *p*-toluenesulfonic acid (Sigma Aldrich, 99%) Amberlyst 36 (Sigma Aldrich).

2.2. Synthesis of H-Sulfo-POSS

Synthesis of H-Sulfo-POSS-1. A modified synthetic procedure for H-Sulfo-POSS was used.²⁷ Octaphenyl-POSS (5 g, 4.8 mmol) was dried *in vacuo* for 5 h inside a Schlenk flask fitted with a stirrer bar. Dichloromethane (35 ml) (dried with 3 Å molecular sieves) was added to make up a suspension. The freely stirring suspension was cooled to 0 °C. Chlorosulfonic acid (10 ml, 150 mmol) was added dropwise

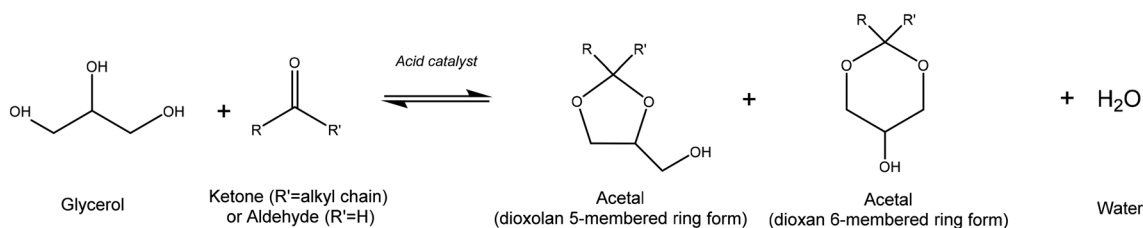


Fig. 2 Overall scheme of the acetalization of glycerol with a ketone or aldehyde.



over the course of 45 min using a dropping funnel. Over the course of the addition of the chlorosulfonic acid the suspension turned into a clear solution. After all had been added, dichloromethane (10 ml) was added, causing a white solid to precipitate. The mixture was allowed to warm to room temperature and was stirred overnight. The next day the precipitate had to be manually broken up. Dichloromethane and excess chlorosulfonic acid were removed under vacuum, first at ambient temperature and later at 90 °C. The remaining solid was suspended in water (200 ml) and Na₂CO₃ was added until the mixture reached a pH of 7. After filtration, the solid was stirred in HCl(aq) (conc., 15 ml), then filtered and washed with water until the filtrate reached a pH of 7. The H-Sulfo-POSS-1 was obtained as a white powder (1.675 g, 30% yield).

¹H-NMR (Sulfo-POSS-1 sodium salt, 400 MHz, D₂O) δ = 7.97 (s, 1H), 7.77 (d, J = 7.3 Hz, 1H), 7.73 (dd, J = 8.0, 1.6 Hz, 1H), 7.46 (t, J = 7.6 Hz, 1H) ppm.

Synthesis of H-Sulfo-POSS-2. Octaphenyl-POSS (4 g, 3.9 mmol) was dried *in vacuo* for 6 h inside a Schlenk-flask fitted with a stirrer bar. Chloroform (80 ml) (freshly distilled from phosphorous pentoxide) was added to make up a suspension of the octaphenyl-POSS. The suspension was cooled to 0 °C before chlorosulfonic acid was added dropwise over the course of 30 min using a dropping funnel. The suspension turned into a clear solution during the addition of the chlorosulfonic acid. The reaction mixture was slowly warmed to room temperature and was stirred overnight. A small amount of white solid had precipitated by the next day. The mixture was cooled to 0 °C before water (10 ml) was added dropwise, which caused precipitation of a white solid. The slurry was diluted with chloroform (40 ml). The solid was separated by filtration and washed with water (50 ml). The white solid was dried *in vacuo* at 50 °C for 6 h. The solid's ion exchange capacity (IEC) was determined by reverse titration. The crude H-Sulfo-POSS product was then stirred in aqueous NaOH (1 eq. based on IEC) to neutralize any remaining sulfuric acid and transform the H-Sulfo-POSS into the corresponding Na-Sulfo-POSS (water soluble). The Na-Sulfo-POSS was then re-acidified by stirring in concentrated aqueous HCl for two days, excess HCl and water was removed *in vacuo*, the resulting solid powder was washed on a filter paper with deionized water before dried *in vacuo*. H-Sulfo-POSS-2 was obtained as fine, white powders.

¹H-NMR (Na-Sulfo-POSS-2, 400 MHz, D₂O) δ = 8.08 (s, 1H), 7.87 (m, 1H), 7.83 (dd, J = 8.1, 1.3 Hz, 1H), 7.58 (m, 1H).

¹³C-NMR (Na-Sulfo-POSS-2, 101 MHz, D₂O) δ = 142.17, 141.59, 137.02, 136.94, 131.59, 130.32, 128.98, 128.41, 126.63, 125.31 ppm.

Synthesis of H-Sulfo-POSS-3. The synthetic procedure was similar to that for H-Sulfo-POSS-2 with the exception that 40 ml of chloroform was used. No precipitate had been formed in the reaction mixture after stirring overnight before being quenched. After reacidification, washing and drying *in vacuo* H-Sulfo-POSS-3 was collected 4.738 g (81% yield).

¹H-NMR (Na-Sulfo-POSS-3, 400 MHz, D₂O) δ = 8.09 (s, 1H), 7.88 (dd, J = 7.5, 1.3 Hz, 1H), 7.83 (dd, J = 8.0, 1.4 Hz, 1H), 7.60 (m, 1H) ppm.

¹³C-NMR (Na-Sulfo-POSS-3, 101 MHz, D₂O) δ = 141.65, 137.00, 136.37, 131.60, 130.33, 128.98, 128.47, 126.79, 125.31 ppm.

2.3. Characterization of H-Sulfo-POSS

Ion exchange capacity and degree of sulfonation. The IEC of any H-Sulfo-POSS material was determined by reverse acid–base titration following previously established protocols involving the use of NaOH and HCl.²⁷ A sample of H-Sulfo-POSS (100 mg) was stirred in NaOH_{aq} (0.05 M, 10 ml) for 30 min. The remaining amount of hydroxide was determined by titration against aqueous HCl (0.01 M) using phenolphthalein as indicator.

NMR spectroscopy. NMR samples were prepared as follows: a sample from the reaction mixture (0.6 g) was quenched by being thoroughly mixed with pyridine (0.15 g). The NMR tube was then prepared with 100 μ l of quenched sample and 500 μ l of D₂O.

ATR-IR spectroscopy. ATR-IR measurements were conducted on solid samples of octaphenyl-POSS and H-Sulfo-POSS-1 using a Bruker Alpha FT-IR spectrometer.

Scanning electron microscopy. SEM images of H-Sulfo-POSS-1, -2 and -3 were recorded on a Hitachi H-S4500 FEG microscope.

2.4. Acetalization of glycerol with 2-butanone and recycling tests

Isolating ketal product. The ketal product was isolated from a reaction mixture. H-Sulfo-POSS-1 (0.129 g) was added to a mixture of glycerol (5 ml) and butanone (30 ml). The mixture was stirred for 2.5 h to achieve a higher conversion of the glycerol. Water was being actively removed using MgSO₄. After filtration, the excess butanone was removed by evaporation under reduced pressure. The remaining ketal was characterized by NMR.

Characterizing reaction mixture by GC-MS. The crude reaction mixture was analyzed by GC-MS to determine the obtained products.

Investigation of the equilibrium yield. Six experiments using different molar ratios of glycerol and butanone were performed to investigate their thermodynamic equilibrium yield. In each experiment glycerol (0.5 g, 5.4 mmol) was first diluted with ethanol (0.8 ml). Butanone (0.5, 1, 3, 6, 8, 13 molar equivalents to glycerol) was then added to the mixture. Finally, the H-Sulfo-POSS-1 catalyst was added, and the reaction mixture was allowed to stir at room temperature overnight. Yield was determined by NMR.

Investigating the catalytic activity of H-Sulfo-POSS. All experiments of this type were performed on the same scale, sampled over time and the only variable was the amount of catalyst being added. In a reaction vessel glycerol (1.0 g, 10.9 mmol) was added, which was diluted with ethanol (1.7 g) to



reduce the viscosity of the medium and allow the magnetic stirrer to operate. Then, 2-butanone (4.7 g, 65.2 mmol, 6 eq.) was added to the vessel and the whole reaction vessel was placed in a stirred water bath, whose temperature was controlled by a thermostat with a precision of ± 0.2 °C. The reaction vessel was left in the bath for 20 min to reach the desired temperature and ensure full mixing and homogeneity of the reactants considering the limited miscibility between glycerol and 2-butanone.³⁴ The catalyst was then added ($t = 0$) and from then on samples (a 0.2 ml) were taken at regular intervals from the reaction mixture. The samples were quickly quenched by an excess of pyridine (0.15 g per 0.60 g sample) to stop them from reacting any further. NMR samples were then prepared according to procedure. A representative example of an ^1H -NMR spectrum from a reaction sample is given in the Fig. S1 (see ESI†).

Centrifugation recycling strategy. Reaction vessels were prepared with a reaction mixture composed exactly as described above. The catalyst was added at $t = 0$ and the reaction mixture was stirred at 25 °C for 150 min. The stirrer bar was then removed, and the glass tube reaction vessel was centrifuged for 25 min at 1500 rpm using a Hettich Universal 16 centrifuge. Carefully the vessels were removed from the centrifuge and the upper three quarters of the reaction mixture was removed from the vessel using a syringe and analyzed by NMR. The bottom quarter was left untouched to be sure that no catalyst sediment would be disturbed and by accident be removed from the vessel. Starting the next cycle, the removed liquid was replenished by fresh reaction mixture.

H-Sulfo-POSS-1 was reapplied for recycling experiments, but this time three tubes were run in parallel. In cycle 1, 5 and 10, the reaction was sampled over time. Because sampling removes catalyst from the reaction mixture it will have to be discarded from future cycles. Therefore, the whole experiment started with three reaction vessels. The first vessel was used up for sample over time experiment in cycle 1, the second and third vessels were used up in sampling over time experiments in cycle 5 and 10 respectively. Fig. 3 presents a summary of the process.

3. Results and discussion

3.1. Synthesis and characterization of H-Sulfo-POSS

H-Sulfo-POSS was synthesized by direct chlorosulfonation of octaphenyl-POSS by adding chlorosulfonic acid in excess at 0 °C, then leaving to react over night at room temperature and finally adding water for hydrolysis. The synthetic protocol that was used was based on that of Kafi *et al.*²⁸ The overall reaction is presented in Fig. 4 below.

The synthesis was performed three times where small changes in parameters were made between them, and which is presented in Table 1 below. The first two experiments resulted in overnight premature precipitation of (product) material, while the third experiment stayed fully dissolved until water was being added the next day. Each of the three different products have been labelled a specific name (H-Sulfo-POSS-1, -2 or -3).

The absence of any acidic contamination material in the collected crude H-Sulfo-POSS product had to be safeguarded as they were to be investigated for their acidic catalytic properties. The crude products were therefore first neutralized with NaOH (Na_2CO_3 was used in the first attempt) and then re-acidified by stirring in concentrated HCl and finally left on high vacuum. During the chlorosulfonation stage, up to eight phenyl groups of each octaphenyl-POSS substrate could have been sulfonated. The collected products therefore contained a varying degree of sulfonation (ratio between sulfonic groups to total number of phenyl groups). The overall degree of sulfonation for each product batch was estimated based on the H-Sulfo-POSS ion-exchange-capacity (IEC) of a sample from that batch. During all three synthetic attempts an initially clear, homogeneous and slightly yellow reaction mixture resulted after all chlorosulfonic acid had been added. Extensive premature precipitation of a white solid occurred over night in the first two experiments. Interestingly these two initial products showed significantly lower IEC than the third, which stayed in solution also until the next day. Some have reported that the degree of sulfonation can be controlled by the excess of chlorosulfonic acid used, where 6–11 equivalents of

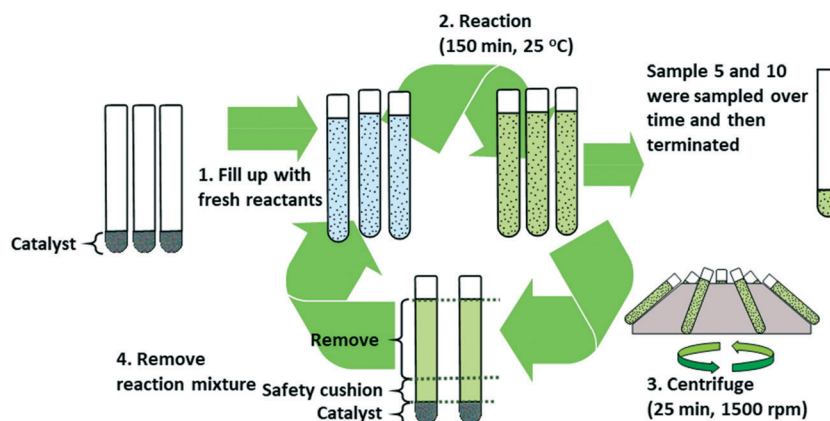


Fig. 3 Operation and catalyst recycling strategy by centrifugation-aided sedimentation after each reaction.



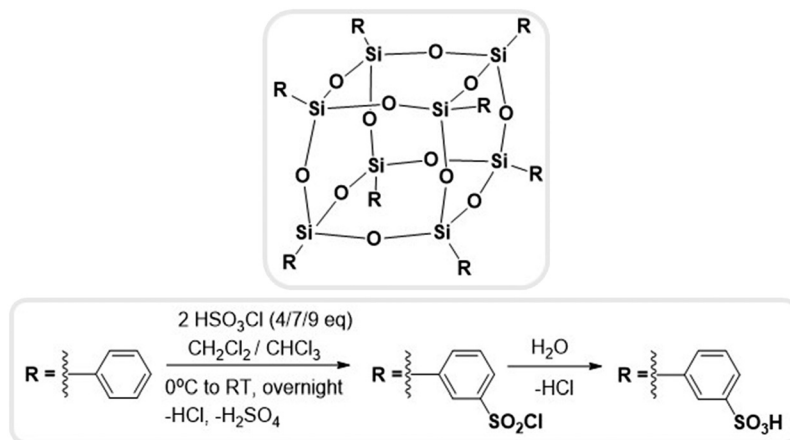


Fig. 4 Synthesis of H-Sulfo-POSS by chlorosulfonation of octaphenyl-POSS and subsequent hydrolysis.

Table 1 The three H-Sulfo-POSS batches presented with the associated conditions, degree of sulfonation and yield. The equivalents are based on the total number of phenyl groups. The yield was calculated by taking the overall sulfonation degree into consideration

H-Sulfo-POSS	Solvent	$V_{\text{(solvent)}}/m_{\text{(OP-POSS)}}$	Eq. of HSO ₃ Cl (per pH)	Est. Sulf. Deg.	Yield
[–]	[–]	[ml g ^{–1}]	[–]	[–]	[%]
1	CH ₂ Cl ₂	9	3.9	0.195	30
2	CHCl ₃	20	7.2	0.285	62
3	CHCl ₃	10	8.7	0.660	81

chlorosulfonic acid to phenyl groups would give about 40% complete sulfonation.²⁹ In contrast, others have reported significantly higher degree of sulfonation when using the same equivalents of chlorosulfonic acid.³⁰ And yet again, others have reported as high as 94% complete sulfonation when only using 1.5 eq. of chlorosulfonic acid to phenyl groups.²⁷ Hence, there is large ambiguity about what the important factors are that determine the degree of sulfonation of octaphenyl-POSS. But in all protocols the temperature has always been kept close to 0 °C while adding the chlorosulfonic acid dropwise. A previous study on sulfonation of phenyl-silanes observed large amounts of Si–C(phenyl) bond cleavage.³¹ In this work the lower degree of sulfonation of the first two products is simply attributed to the premature precipitation from the reaction mixture. This effectively made their still unreacted phenyl groups inaccessible to the chlorosulfonic acid. The risk of premature precipitation from the reaction mixture seems to increase when more solvent (chloroform or DCM) is used per amount of OP-POSS.

The product that was collected from experiment 3 had an overall degree of sulfonation of 66% after having reacted at room temperature for 12 h. Hence, the rate of the sulfonation reaction itself at room temperature was not very vigorous at all. To reach higher degrees of sulfonation it is certainly important to maintain full solubility through the first stage (hence use a large excess of chlorosulfonic acid), but longer reaction times and slightly increased reaction temperatures are suggested to be tested. All three H-Sulfo-POSS products were obtained as very fine grey/white powders. They were

practically insoluble in any of the following solvents (water, ethanol, DMSO, THF, DCM, chloroform). And so, their characterization by NMR had to be done on their associated Na-salts by reacting the H-Sulfo-POSS materials with NaOH.²⁹ Which improved solubility in water for H-Sulfo-POSS-1 to 2 g L^{–1}, and for H-Sulfo-POSS-2 and -3 to approximately 5 g L^{–1}. The yields of the products were not great for any of the experiments, especially bad for H-Sulfo-POSS-1 (30%). The reason for this is mainly due to underestimating the water solubilities of the Na-derivatives during their washing with water. Albeit those steps were necessary to take as to guarantee no remainder of chlorosulfonic, H₂SO₄ or HCl being present in the final products.

Ion exchange capacity and degree of sulfonation. To determine the IEC of the different H-Sulfo-POSS products, a reverse acid–base–titration was carried out using NaOH and HCl according to previous work on H-Sulfo-POSS.^{27,29} IEC was determined for both the crude product and the product obtained after the neutralization–re-acidification step. The results are presented in Table 2 below.

Table 2 Ion exchange capacity (IEC) of the different H-Sulfo-POSS products

H-Sulfo-POSS	IEC [meq g ^{–1}]		Sulfonation degree of reacidified H-Sulfo-POSS materials
[–]	Crude	Reacidified	
1	—	1.34	0.195
2	2.99	1.89	0.285
3	4.03	3.62	0.660



As can be seen, the crude products had significantly greater IEC than after they had been neutralized and re-acidified again. The reason for this is that contaminating H_2SO_4 , HCl or chlorosulfonic acid remaining in the crude products would by then have been neutralized and removed. But it is also possible that the re-acidification process was not complete and that there existed unprotonated sulfonic acid groups after the re-acidification step. This could be a possibility as when the relatively highly water-soluble Na-Sulfo-POSS is protonated, its solubility decreases and starts precipitating and trapping still yet unprotonated sulfonic groups inside precipitated particles.

NMR spectroscopy. All of the synthesized H-Sulfo-POSS had very limited solubility in any of the solvents tested (MeOH , H_2O , toluene, CHCl_3) and so the associated sodium salts (Na-Sulfo-POSS) were used to make up solutions in water which were analyzed by ^1H , ^{13}C and ^{29}Si -NMR. The ^1H -NMR spectra of Na-Sulfo-POSS-1, -2 and -3 are presented in Fig. S2 of the ESI†

The assignment of the spectra was not trivial as each sample contained a mixture of Sulfo-POSS molecules with a variety of different degrees of sulfonation. The singlet at 8.04 represents the proton at the *ortho*-position to both POSS and the sulfonic group.^{28,29} The peaks slightly downfield were not possible to be individually identified due to peak overlap of protons associated with both sulfonated and non-sulfonated phenyl groups.

ATR-IR spectroscopy. The starting material octaphenyl-POSS (OP-POSS) and the product H-Sulfo-POSS-1 were analyzed by ATR-FTIR-spectroscopy in their solid state. The spectra that were obtained are presented in Fig. 5.

The IR spectrum of the starting material (OP-POSS) shows some distinguishable bands that were identified as belonging to aromatic $\text{C}=\text{C}$ and $\text{C}-\text{H}$ stretch vibrations (around 3025 cm^{-1}), $\text{Si}-\text{C}$ -bending vibrations (at 1425 cm^{-1}) and $\text{Si}-\text{O}-\text{Si}$ stretching vibrations (at 1086 and $750\text{--}800\text{ cm}^{-1}$). After the aromatic electrophilic sulfonation a few very distinguishable bands associated with the $-\text{SO}_3\text{H}$ group (1050 , 1120 and 1170 cm^{-1}) appeared.³² Also, the broad band at 3370 cm^{-1} can be attributed to $\text{O}-\text{H}$ stretching absorption bands, indicating strong H -bonding by its broad shape. The band at around 1650 cm^{-1} is attributed to the *meta*-substitution of the phenyl rings of octaphenyl-POSS.²⁹ The spectra have not been scaled and can only be interpreted qualitatively and not quantitatively.

Scanning electron microscopy. A field emission scanning electron microscopy (FE-SEM) was used for taking high resolution pictures of the H-Sulfo-POSS-1, H-Sulfo-POSS-2 and H-Sulfo-POSS-3. These images are presented in Fig. 6.

The H-Sulfo-POSS-1 compound forms particles of varying sizes from as small as $9\text{ }\mu\text{m}$ up to approximately $250\text{ }\mu\text{m}$, where the larger particles look like a very compact and consistent assembly of smaller particles. At the maximum zoom on the particles, the surface looks highly uneven and rough, showing a high degree of porosity. A similar scenario is observed with the H-Sulfo-POSS-2 material, in which the

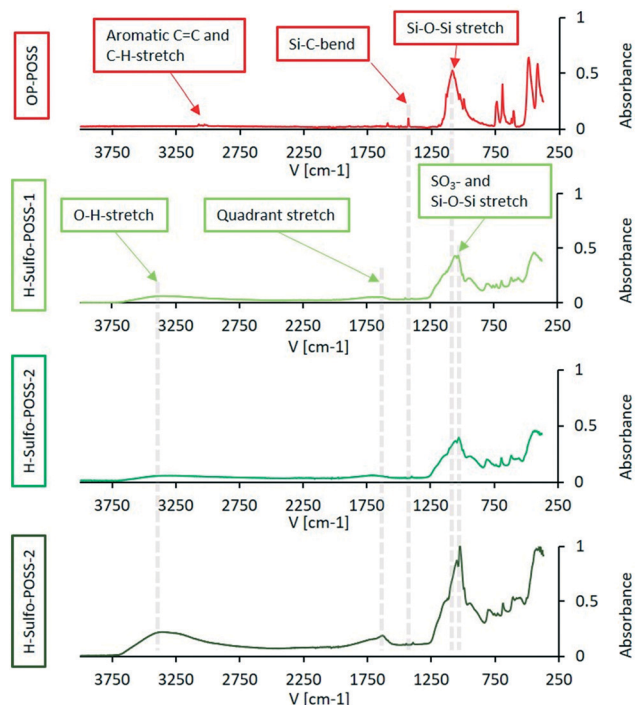


Fig. 5 ATR-FTIR spectra of octaphenyl-POSS (OP-POSS) and the three H-Sulfo-POSS catalysts.

roughness appears to give high access to the active catalytic sites. The H-Sulfo-POSS-3 material shows significant amounts of very fine particles scattered at the $2\text{ }\mu\text{m}$ and 800 nm zoom.

3.2. Catalytic tests of H-Sulfo-POSS in the acetalization of glycerol with butanone

Equilibrium yield. The acetalization of glycerol is an equilibrium reaction that is highly dependent upon the excess of ketone or aldehyde to glycerol. Previous studies have also shown its dependence on temperature, but the excess of the carbonyl-containing reactant is far more relevant.^{17,33} Thus, the maximum achievable conversion and yield is strongly dependent on the ratio between glycerol and 2-butanone in our case. To find a suitable ratio that gives a good conversion to allow reaction monitoring over time to be implemented, a set of six experiments were conducted in which the butanone to glycerol molar ratio varied between 0.5/1 to 13/1. The equilibrium yields reached for each of the six experiments is presented in Fig. 7.

As may be observed, the molar excess of 2-butanone significantly affects the equilibrium, as observed with other aldehydes and ketones in other acetalization reactions.¹⁰ For the future experimental protocol it was decided that a glycerol/butanone ratio of 1:6 was suitable where a maximum yield of 82.3% at equilibrium is to be expected. Ethanol was identified as a suitable solvent for the otherwise immiscible glycerol and ketones³⁴ to become fully miscible. This is important to avoid mass transfer limitations owing to the presence of two liquid phases during the first moments



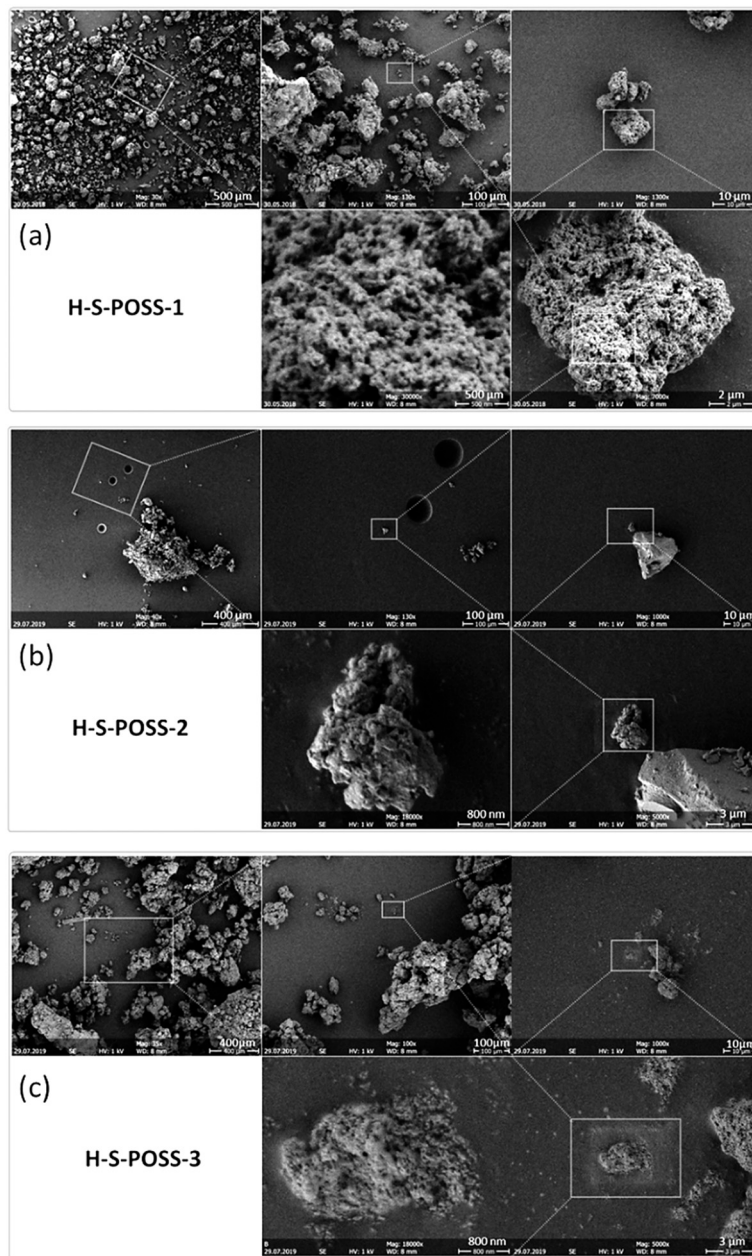


Fig. 6 Field emission scanning electron microscopy (FE-SEM) pictures of the prepared catalysts. (a) H-Sulfo-POSS-1; (b) H-Sulfo-POSS-2 and (c) H-Sulfo-POSS-3.

of the reaction. Also, using the additional solvent ethanol has shown not to affect the equilibrium conversion of the reaction³³ since it does not compete for the acetalization reaction. This would require the presence of two –OH groups (such as in the case of glycerol or glycols); thus, having only one –OH, ethanol would only form a hemiacetal, which are very unstable species and are indeed not observed.³⁵

Catalytic activity. In order to operate under the mildest conditions possible, 25 °C was selected as temperature for our studies. The three H-Sulfo-POSS catalysts were then applied in the ketalisation of glycerol with butanone, taking samples from the reaction mixture at regular intervals over time. H-Sulfo-POSS can be viewed as a molecular weight enlarged multifunctional

version of benzenesulfonic acid, with *para*-toluenesulfonic acid (PTSA) as closest, widely available and utilized derivative. Conventional heterogenized versions of PTSA are the Amberlyst type ion exchange resins, such as Amberlyst 36, used in this work. The catalytic activity of H-Sulfo-POSS was therefore compared with that of PTSA and Amberlyst-36. The catalysts were applied at a loading of 0.1 mol% (mol_H/mol_{gly}) acid protons relative to glycerol. The results from that set of experiments is presented in Fig. 8 below.

The higher degree of sulfonation gave a more active catalyst as can be seen from the relative order in activity between H-Sulfo-POSS-1, -2 and -3. This may be a consequence of an enhanced interaction between the



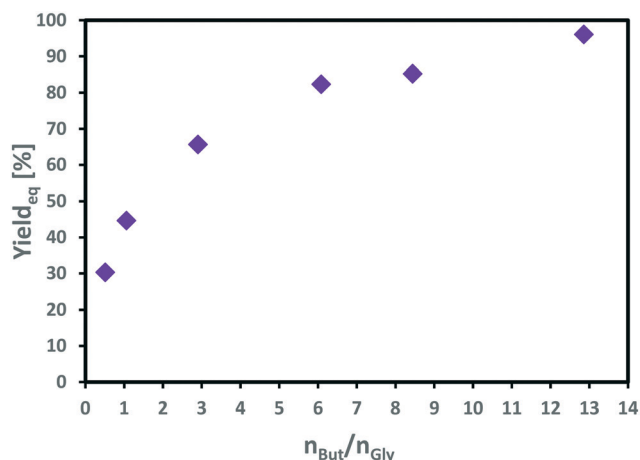


Fig. 7 The equilibrium yield in the ketalisation of glycerol with butanone at different molar ratios. Conditions: 16 h, 25 °C, ethanol (0.8 ml), glycerol (0.5 g, 5.4 mmol), butanone (according to ratio), catalyst: H-Sulfo-POSS-1 (1 mol%).

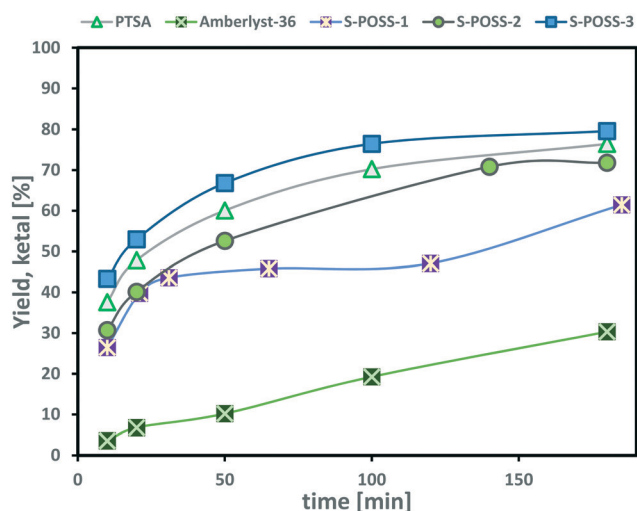


Fig. 8 Reaction profiles for the ketalisation of glycerol with butanone using PTSA, Amberlyst-36, H-Sulfo-POSS-1, -2 and -3 as catalysts. Conditions: 25 °C. Ethanol (1.7 g), glycerol (1 g, 10.8 mmol), butanone (4.7 g, 65.2 mmol, 6 equiv. per glycerol), catalyst loading of 0.1 mol% ($\text{mol}_{\text{H}^+}/\text{mol}_{\text{gly}}$).

substrates and catalyst due to a higher presence of SO_3^- moieties that initiate the reaction mechanism with the

hydroxyl functions of glycerol.³⁵ H-Sulfo-POSS-3 presents similar or even slightly better activity than PTSA. Amberlyst-36 indeed presents a lower activity, undoubtedly caused by mass transfer limitations into its porous structure.

Additionally, as seen in Table 3, the TOF of our synthesized catalysts is much higher than an industrial reference ion exchange resin like Amberlyst 36 and also a molecular reference catalyst like PTSA. There is not an abundance of studies on the acetalization reaction between glycerol and butanone, and none that shows any reaction profiles or TOF. In contrast to other works in literature with catalysts like the heteropolyacid $\text{H}_3\text{PW}_{12}\text{O}_{40}$ (ref. 21) and with rhenium supported on silica,²⁴ the activity in terms of TOF appears to be higher. This is remarkable, considering that the reaction conditions employed in the other cases were more favourable. In one case the molar excess of butanone to glycerol is as high as 20,²⁴ which makes the contact between butanone and glycerol more favourable as the dispersed droplets of the latter are significantly smaller (*i.e.*, there is a larger interfacial area) than when using lower molar excesses.³⁶ In the other case, the molar excess of butanone is also higher, but more relevantly for catalytic activity, the temperature is 328 K compared to our experiments at room temperature (298 K).²⁴ However, it should be noted that in the mentioned references^{21,24} the yield of the acetal product was measured at high conversions of glycerol, close to the thermodynamic equilibrium of the reaction,²⁴ which is far too high to measure meaningful TOFs.

Recycling by centrifugation. Because the H-Sulfo-POSS catalyst had extremely poor solubility in the reaction mixture or in other solvents like water, ethanol, methanol, toluene, DCM (data not shown here) it was hypothesized that centrifugation could be a means for catalyst recovery. To investigate this, the H-Sulfo-POSS catalysts were applied in the ketalisation reaction for a time of 180 min, the reaction mixture was then centrifuged, product reaction mixture was decanted, and fresh substrate was added. This cycle was repeated 10 times to investigate if the yield of the ketal would change. The recycling experiments were conducted with the catalysts H-Sulfo-POSS-1, -2, and -3. The yield of ketal at the end of each reaction and centrifugation cycle for each catalyst is presented in Fig. 9.

The H-Sulfo-POSS-3 catalyst initially gave the highest yield of the ketal as expected from the TOF values shown in

Table 3 Comparison of the activity and reaction conditions used in the synthesis of the glycerol ketal with other literature references

Catalyst	<i>T</i> (K)	Molar excess ketone: butanone	Glycerol conversion ^a (%)	TOF (h^{-1})	Ref.
H-Sulfo-POSS-1	298	6	26.5	1587	This work
H-Sulfo-POSS-2	298	6	30.7	1844	This work
H-Sulfo-POSS-3	298	6	43.4	2601	This work
Amberlyst 36	298	6	3.6	213	This work
PTSA	298	6	37.6	2256	This work
Re/SiO ₂	328	10	92.6	115	24
H ₃ PW ₁₂ O ₄₀ ^b (1 mol%)	298	20	74	70.7 ^c	21

^a Glycerol conversion at which the TOF was calculated. ^b H₃PW₁₂O₄₀ = heteropolyacids. ^c Calculated from the data in the reference.



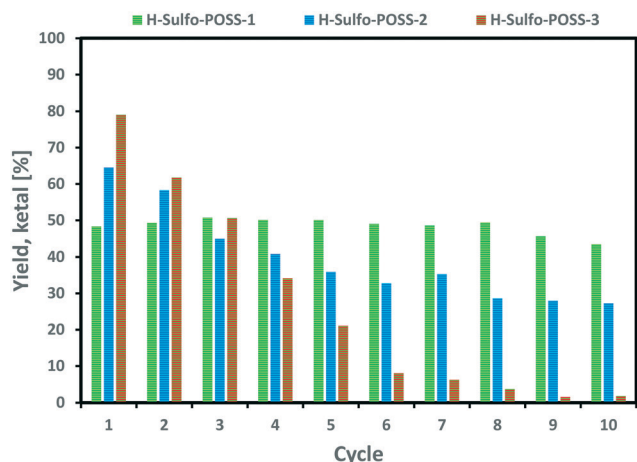


Fig. 9 Yield per recycle run for the H-Sulfo-POSS catalysts using the centrifugation approach. Conditions: 25 °C, 150 min, ethanol (1.7 g), glycerol (1 g, 10.8 mmol), butanone (4.7 g, 65.2 mmol, 6 equiv. per glycerol), H-Sulfo-POSS catalysts loaded at 0.1% ($\text{mol}_{\text{H}^+}/\text{mol}_{\text{gly}}$).

Table 3. However, with each cycle the yield of the ketal was rapidly decreasing. H-Sulfo-POSS-2 showed an intermediate high initial yield of ketal with a significant but limited drop in the yield for the first few cycles. The H-Sulfo-POSS-1 catalyst showed an intermediate initial yield of the ketal of about 50%; however, this yield remained almost unchanged throughout 10 cycles. Obviously, H-Sulfo-POSS-3, which shows the highest solubility of the three H-Sulfo-POSS catalysts, will be washed out relatively easily. This is expected in H-Sulfo-POSS materials whose sulfonation degree is higher than 50% (ref. 29) as is the case of H-Sulfo-POSS-3, which exhibits 66% as indicated in Table 2. In case of a soluble catalyst like H-Sulfo-POSS-3 separation by membrane filtration with an appropriate pore size could be an alternative procedure to be assessed.

The H-Sulfo-POSS-1 catalyst was further investigated in recycling experiments whereby sample over time experiments were performed either at the start (cycle 1), at the 5th cycle or at the 10th cycle. A sample over time experiment is essentially equivalent to a destructive sample. Therefore, the recycling experiment setup started with three reaction vessels running in parallel, when a time-resolved experiment had to be conducted that reaction vessel was terminated from further recycling runs as sampling removes significant portions of catalyst from the reaction mixture. The results from those experiments are presented in Fig. 10.

The reaction profile is very similar in cycle 1, 5 and 10 and in all three instances showing a more active system than that based on the Amberlyst-36 catalyst.

4. Conclusions

Three batches of sulfonated octaphenyl-POSS, H-Sulfo-POSS, were synthesized, each of which with a slightly higher degree of sulfonation. The H-Sulfo-POSS catalysts were characterized by NMR, IR and SEM. The IEC was measured for all H-Sulfo-

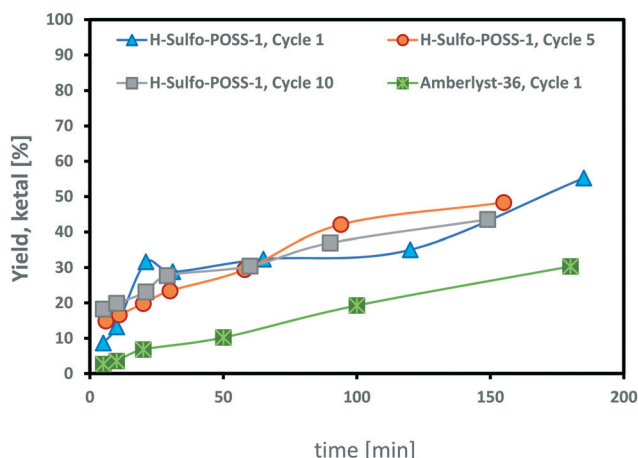


Fig. 10 Reaction profile of the ketalisation of glycerol using fresh and recycled H-Sulfo-POSS as catalyst and comparison with Amberlyst 36. Conditions: 25 °C, 150 min, ethanol (1.7 g), glycerol (1 g, 10.8 mmol), butanone (4.7 g, 65.2 mmol, 6 equiv. per glycerol), H-Sulfo-POSS-1 catalysts loaded at 0.1% ($\text{mol}_{\text{H}^+}/\text{mol}_{\text{gly}}$).

POSS catalysts to determine their degree of sulfonation. The solubility of the H-Sulfo-POSS was extremely low in all the solvents that were investigated. The Na-Sulfo-POSS on the other hand was slightly soluble in water and other polar solvents, which then allowed them to be analyzed by NMR. The H-Sulfo-POSS compounds were investigated for their catalytic activity in the ketalisation reaction of glycerol with butanone. The catalytic activity of each of the synthesized H-Sulfo-POSS catalysts in this reaction increased with the degree of sulfonation, the most active catalyst, H-Sulfo-POSS-3 showing a TOF as high as 2601 h^{-1} . The activity of H-Sulfo-POSS-2 and -3 was similar to PTSA while H-Sulfo-POSS-1 was somewhat less active albeit still considerably more active than the industrial reference Amberlyst-36. This is explained by the higher ion exchange capacity that these modified nanocomposites exhibit as the charge density is increased with a higher degree of sulfonation. Centrifugation was explored as a way of recycling the H-Sulfo-POSS catalysts. H-Sulfo-POSS-1 showed good recyclability over 10 centrifugation-recycling runs, which is explained by the lower solubility of H-Sulfo-POSS-1 as compared to H-Sulfo-POSS-2 and -3. These sulfonated materials show an outstanding prospects for biomass conversion to value-added products and other biofuels in other reactions starting from glycerol, such as esterifications and etherifications, or sugars, like the dehydration to furans. Further work could lead to modifying the POSS material and then functionalizing them to tune their solubility and activity. In addition, due to their size, there is potential catalyst recycling employing membrane technologies.

Author contributions

Viktor Söderholm: conceptualization, data curation, formal analysis, investigation, methodology, visualization, writing-original draft, writing-review & editing. Jesús Esteban: conceptualization, data curation, formal analysis,



supervision, visualization, writing-original draft; writing-review & editing. Dieter Vogt: conceptualization, funding acquisition, methodology, project administration, resources, supervision, writing-review & editing.

Conflicts of interest

There are no conflicts to declare.

Acknowledgements

Gefördert durch die Deutsche Forschungsgemeinschaft (DFG) – TRR 63 “Integrierte chemische Prozesse in flüssigen Mehrphasensystemen” (Teilprojekt D3) – 56091768.

References

- G. Li, L. Wang, H. Ni and C. U. Pittman, *J. Inorg. Organomet. Polym.*, 2001, **11**, 123–154.
- W. Zhang, G. Camino and R. Yang, *Prog. Polym. Sci.*, 2017, **67**, 77–125.
- X. Chen and L. F. Dumée, *Adv. Eng. Mater.*, 2019, **21**, 1800667.
- W. Zhang and A. H. E. Müller, *Prog. Polym. Sci.*, 2013, **38**, 1121–1162.
- S. Mohapatra, T. Chaiprasert, R. Sodkhomkhum, R. Kunthom, S. Hanprasit, P. Sangtrirutnugul and V. Ervithayasuporn, *ChemistrySelect*, 2016, **1**, 5353–5357.
- A. Akbari, A. Naderahmadian and B. Eftekhari-Sis, *Polyhedron*, 2019, **171**, 228–236.
- A. Falk, J. M. Dreimann and D. Vogt, *ACS Sustainable Chem. Eng.*, 2018, **6**, 7221–7226.
- A. Behr, J. Eilting, K. Irawadi, J. Leschinski and F. Lindner, *Green Chem.*, 2008, **10**, 13–30.
- C. H. C. Zhou, J. N. Beltramini, Y. X. Fan and G. Q. M. Lu, *Chem. Soc. Rev.*, 2008, **37**, 527–549.
- A. Cornejo, I. Barrio, M. Campoy, J. Lazaro and B. Navarrete, *Renewable Sustainable Energy Rev.*, 2017, **79**, 1400–1413.
- A. R. Trifoi, P. S. Agachi and T. Pap, *Renewable Sustainable Energy Rev.*, 2016, **62**, 804–814.
- V. R. Ruiz, A. Vely, L. L. Santos, A. Leyva-Pérez, M. J. Sabater, S. Iborra and A. Corma, *J. Catal.*, 2010, **271**, 351–357.
- N. Suriyaprapadilok and B. Kitiyanan, *Energy Procedia*, 2011, **9**, 63–69.
- R. R. Pawar, S. V. Jadhav and H. C. Bajaj, *Chem. Eng. J.*, 2014, **235**, 61–66.
- P. H. R. Silva, V. L. C. Gonçalves and C. J. A. Mota, *Bioresour. Technol.*, 2010, **101**, 6225–6229.
- J. Esteban, F. Garcia-Ochoa and M. Ladero, *Green Process. Synth.*, 2017, **6**, 79–89.
- J. Esteban, M. Ladero and F. Garcia-Ochoa, *Chem. Eng. J.*, 2015, **269**, 194–202.
- J. Deutsch, A. Martin and H. Lieske, *J. Catal.*, 2007, **245**, 428–435.
- H. Serafim, I. M. Fonseca, A. M. Ramos, J. Vital and J. E. Castanheiro, *Chem. Eng. J.*, 2011, **178**, 291–296.
- Y. Leng, J. Zhao, P. Jiang and D. Lu, *Catal. Sci. Technol.*, 2016, **6**, 875–881.
- M. J. da Silva, A. A. Julio and F. C. S. Dorigetto, *RSC Adv.*, 2015, **5**, 44499–44506.
- M. J. da Silva, M. de Oliveira Guimaraes and A. A. Julio, *Catal. Lett.*, 2015, **145**, 769–776.
- S. Guidi, M. Noe, P. Riello, A. Perosa and M. Selva, *Molecules*, 2016, **21**, 657.
- M. Kapkowski, W. Ambrozkiewicz, T. Siudyga, R. Sitko, J. Szade, J. Klimontko, K. Balin, J. Lelątko and J. Polanski, *Appl. Catal., B*, 2017, **202**, 335–345.
- J. Esteban, A. J. Vorholt and W. Leitner, *Green Chem.*, 2020, **22**, 2097–2128.
- S. Van de Vyver, J. Thomas, J. Geboers, S. Keyzer, M. Smet, W. Dehaen, P. A. Jacobs and B. F. Sels, *Energy Environ. Sci.*, 2011, **4**, 3601–3610.
- D. Aili, T. Allward, S. M. Alfaro, C. Hartmann-Thompson, T. Steenberg, H. A. Hjuler, Q. Li, J. O. Jensen and E. J. Stark, *Electrochim. Acta*, 2014, **140**, 182–190.
- A. Kafi, Q. Li, T. Chaffraix, J. Khoo, T. Gengenbach and K. J.-C. Magniez, *Polymer*, 2018, **137**, 97–106.
- S. Subianto, M. K. Mistry, N. R. Choudhury, N. K. Dutta and R. Knott, *ACS Appl. Mater. Interfaces*, 2009, **1**, 1173–1182.
- C. Hartmann-Thompson, A. Merrington, P. I. Carver, D. L. Keeley, J. L. Rousseau, D. Hucul, K. J. Bruza, L. S. Thomas, S. E. Keinath, R. M. Nowak, D. M. Katona and P. R. Santurri, *J. Appl. Polym. Sci.*, 2008, **110**, 958–974.
- E. Carlier, A. Revillon, A. Guyot and P. Baumgartner, *React. Polym.*, 1993, **21**, 15–25.
- B. Decker, C. Hartmann-Thompson, P. I. Carver, S. E. Keinath and P. R. Santurri, *Chem. Mater.*, 2010, **22**, 942–948.
- M. R. Nanda, Z. Yuan, W. Qin, H. S. Ghaziaskar, M.-A. Poirier and C. C. Xu, *Fuel*, 2014, **117**, 470–477.
- J. Esteban, A. J. Vorholt, A. Behr, M. Ladero and F. Garcia-Ochoa, *J. Chem. Eng. Data*, 2014, **59**, 2850–2855.
- V. Calvino-Casilda, K. Stawicka, M. Trejda, M. Ziolek and M. A. Bañares, *J. Phys. Chem. C*, 2014, **118**, 10780–10791.
- H. Murasiewicz and J. Esteban, *Ind. Eng. Chem. Res.*, 2019, **58**, 6933–6947.

